Quasiequilibrium multistate cellular automata

Federico G. Pazzona *
Dipartimento di Chimica e Farmacia, Università degli Studi di Sassari, via Vienna 2, 07100 Sassari, Italy

Giovanni Pireddu
PASTEUR, Département de Chimie, École Normale Supérieure, PSL University, Sorbonne Université, CNRS, 75005 Paris, France

Pierfranco Demontis
Dipartimento di Chimica e Farmacia, Universitá degli Studi di Sassari, via Vienna 2, 07100 Sassari, Italy

(Received 23 November 2021; accepted 4 January 2022; published 18 January 2022)

In our effort to tackle the problem of letting nontrivial interactions, thermodynamic equilibrium, and full synchronicity coexist, and in the hope of reviving interest in cellular automata as promising tools for the quantitative, large-scale investigation of multiparticle systems, we built a fully synchronous cellular automaton rule for the simulation of occupancy-based lattice systems with multistate cells and neighboring interactions. The core of this rule, which constitutes an actual synchronous sampling scheme, is a negotiation stage; it produces cell occupancy distributions in very good agreement with their sequential Monte Carlo counterparts, and it satisfies a cellwise detailed balance principle thanks to the use of "mixed" intermediate states that allow for the computation of locally averaged acceptance probabilities. We took a square lattice (but the rule itself is not bound by dimensionality) as a basis for comparison with sequential Monte Carlo for showing that this synchronous rule leads to quasiequilibrium; the fulfillment of cellwise detailed balance is shown through results obtained for a small one-dimensional system, where the transition matrix could be computed exactly.

DOI: 10.1103/PhysRevE.105.014116

I. INTRODUCTION

In their original formulation, cellular automata (CA) are homogeneous lattices of discrete states, where at each time step the state of each cell in the lattice is updated according to an updating rule which is a function of the state itself and of the state of neighboring cells; all the cells are updated synchronously, and the updating rule can be either deterministic or probabilistic, depending on whether random numbers are used [1,2]. Especially during the 1980s and the 1990s, CA received a remarkable amount of attention from the scientific community due to their computational efficiency and high versatility in mimicking a wide range of physical phenomena, especially those regarding self-organization and nonequilibrium phase transitions, while working with a relatively low number of degrees of freedom [1,3,4]. Dedicated computational environments were also developed that were based entirely upon CA [5], and in the realm of simulation methods for physical sciences, CA inspired the development of dissipative particle dynamics (DPD) [6–8] and lattice Boltzmann methods [9,10].

Although probabilistic CA are suitable for Markov chain modeling, the high level of attention dedicated to CA perhaps started fading in the late 2000s. In our opinion, one of the reasons for this is the following: when it comes to the sampling of given (nontrivial) distributions, synchronous CA may turn out to be wild beasts to tame. Due to synchronicity itself, it is impossible to formulate trial moves for single cells and then to apply the importance sampling criterion like we do in equilibrium Monte Carlo (MC) simulations. Therefore, it is hard to impose detailed balance on synchronous CA models; a much easier way to do it is to abandon the idea of full synchronicity and to resort to partitioning and/or asynchronicity instead. In fact, detailed balance, nontrivial (even though still local) interactions, and full synchronicity hardly coexist. In the very rare cases in which such coexistence is realized, we face a situation that is conceptually very different from the MC case: when we work with MC, we are the ones who impose detailed balance in order to drive the system towards the equilibrium distribution we want, through a Markov chain; when we work with CA instead, we cannot choose the mathematical form of the equilibrium distribution sampled—in other words, we cannot implement any potential function we want, like we do with MC; the coexistence of synchronicity and detailed balance causes the CA we are working with to obey one particular (so-called) "pseudo-Hamiltonian"; we must stick with it, and that is it [11–15].

The literature on this topic is not only very limited, but it also seems to be totally lacking in the development of methods and strategies aimed at letting a fully synchronous update of the cells *coexist* with multistate cells (i.e., cells whose state can take an arbitrary number of values, rather than just two) and with thermodynamic equilibrium in the presence of nontrivial interactions. Some multiparticle models

* fpazzona@uniss.it

that are actually able to reach thermodynamic equilibrium under certain conditions have been investigated [1], but they are characterized by the *absence* of interactions—they have been used in hydrodynamics problems, but they almost vanished from the literature not long after the introduction and refinement of DPD.

It is curious that efforts to discover more about multistate, synchronous CA have virtually ground to a halt—at least for the representation of equilibrium systems. We find it curious, because both the words *multistate* and *synchronous* are still alive in computational physics, and both of them refer to native features of CA. The word "multistate," referring to each cell of a lattice, can be expressed also as *multiparticle*—which means that having access to a theory on "equilibrium in multiparticle, interacting CA" would turn out very useful in some applications: for example, multiparticle models [16–20] may emerge naturally from spatial coarse-graining procedures [4,21–28], where effective multiparticle interactions are extracted from molecular-scale simulation data (e.g., from grand canonical Monte Carlo simulations [29–36]); to have the chance to implement such interactions directly on a synchronous lattice would prove useful in experimenting with the behavior of the coarse-grained version of the system under study on much larger scales of space and time. Turning to the word "synchronous," when it is used to refer to a computational practice, it surely implies *parallel*, thus suggesting that a simulation model that is natively parallel, like the CA, would lend itself better to implementation on a parallel architecture; now, the growing use of graphics processors for the implementation of parallel algorithms [37,38], together with the remarkable number of parallelization schemes specifically designed for Monte Carlo simulations [39], suggests that the need for better and better parallel methods is still there, just as it was there at that time in the 1980s and 1990s when CA were so intensely investigated, but now it seems to us that the problems posed by the conflict between synchronicity and detailed balance somehow turned out to be discouraging enough to cause the search for parallel methods to end up going by routes other than CA modeling.

However, besides the purely "applicative" motivations related to the "multiparticle" and the "parallel" features of the CA that we investigate in this work, and also besides our unconcealed hope of reviving interest in cellular automata as promising tools for the quantitative investigation of multiparticle systems, there is another fact that constitutes a valid reason for us to keep on believing that finding a protocol for the construction of fully synchronous equilibrium CA rules is still worth the pain of searching for it. That is, in order to let full synchronicity work in a discrete lattice along with thermodynamic equilibrium and nontrivial interactions, one might end up by exploring new territories in the realm of sampling strategies, i.e., the all of the known sampling techniques in computational physics may be just the tip of the iceberg.

In this work, we show a possible way to let fully synchronous CA produce a stationary distribution in very good agreement with a given (local) potential function. To achieve this task, we build a CA where, at each time step, every cell proposes a new state (*proposal substep*); once all the cells have made their proposals, every one of them is accepted or rejected according to a probability that is a function of a combination between the proposals made by neighboring cells (*acceptance/rejection substep*). Such a combination of proposals corresponds to an intermediate state, or better yet, an "intermediate situation." which we will call a *mixed intermediate state*. Intermediate states are used in biased MC sampling to improve acceptance [40–42]; the key feature of each mixed intermediate state here is that it can be reached with the same probability both from the global departure state (i.e., the state that all cells have right before the proposal substep) and from the global arrival state (i.e., the state that all cells have right after the acceptance/rejection substep).

II. THE REFERENCE MODEL

We will refer to a model made of a square grid of N cells, with neighboring interactions. Every cell can host up to K particles (i.e., it can have a state, or *occupancy*, in the set $\{0, 1, \ldots, K\}$); the self-interaction energy of a cell, cell i, for example, with occupancy n_i, is identified with $\varepsilon(n_i)$. We denote by $\mathcal{L}_i$ the list of its ν neighbors; around i we can locate four neighbors of one kind (neighborhood class A), with which i shares an edge, and four neighbors of another kind (neighborhood class B), with which i shares a corner. If with X we indicate the neighboring class, then $\mathcal{L}_{iX}$ is the list of the ν_X neighbors of class X, $\nu = \nu_A + \nu_B$, and $\mathcal{L}_i = \mathcal{L}_{iA} \cup \mathcal{L}_{iB}$. If $j \in \mathcal{L}_{iX}$ is an X-class neighbor of i and has occupancy n_j, then we indicate as $\phi_X(n_i, n_j)$ the energy of interaction between i and j. Let us assume that temperature, T, and chemical potential, μ, are held fixed throughout the whole system; then the system potential is

$$\Omega_{\text{tot}} = \sum_i [-\mu n_i + \varepsilon(n_i)] + \frac{1}{2} \sum_i \sum_X \sum_{j \in \mathcal{L}_{iX}} \phi_X(n_i, n_j). \quad (1)$$

III. THE SYNCHRONOUS MODEL

We will now proceed with describing in detail *one time step* of the algorithm.

(*i*) *Transition proposals.* Every cell, say cell i, proposes a transition from occupancy n_i to either occupancy $n_i - 1$ or $n_i + 1$, at random. If we indicate the transition with Δ_i, we have

$$\Delta_i = \pm 1, \quad \text{proposed with probability} \quad q^{(\pm)},$$

where $q^{(+)} = q^{(-)} = \frac{1}{2}$. On the basis of some criteria that we are going to discuss, the proposed transition can be accepted or rejected (rejection corresponds to the null transition: if a cell proposal is rejected, its occupancy does not change). At this stage, transitions that would bring occupancies to the unrealistic values of -1 or $K + 1$ are still allowed—they would be automatically rejected at a later stage. All cells make their proposals at the same time, independently of one another, and at this stage they do not change their state: they just propose a transition.

(*ii*) *Neighborhood scenarios and the mixed intermediate state.* Let us consider cell i and its neighborhood. Up to now, no cell changed its occupancy, but all cells (including i and its neighbors) have just made their transition proposals, which can be listed in $\{\Delta_j\}_{j \in \mathcal{L}_i}$. Therefore, in the neighborhood of i a number of possible scenarios emerge, i.e., a number of sets of

possible post-transition occupancies. Just to give an example, let us pick the first three neighbors of cell i, i.e., the first three cells in the $\mathcal{L}_i$ list. In one of the possible scenarios in which three such cells are present, all their transition proposals are rejected; in another scenario, only the first of the three has its proposal accepted; and in another scenario, the first and the second neighbors have their proposals accepted; and so on and so forth, until all the 2^3 possible combinations are covered. If we consider all the ν cells that make the neighborhood of i, then we have 2^ν possible neighborhood scenarios; nevertheless, depending on how the lattice connections are structured, 2^ν may turn out to be a very large number, thus making the computation of all possible scenarios very expensive. To keep the computation efficient, we consider "reduced" scenarios, that is, scenarios made by a *subset* of $\mathcal{L}_i$, this subset being made by only d neighboring, randomly selected cells (with $d \leqslant \nu$). According to this definition, every scenario in the neighborhood of i is an array with d entries. Now, we already used i to indicate one cell, and j to indicate its neighbors; we can use the letter k (with $k = 1, \ldots, 2^d$) to indicate the possible scenario. We define the kth neighborhood scenario as

$$\boldsymbol{\sigma}_{ik} = \{\sigma_{ik1}, \ldots, \sigma_{ikd}\},$$

where every σ_{ikj} is either $n_j + \Delta_j$ (i.e., the post-transition occupancy that j would assume if its proposal were *accepted*) or n_j (i.e., the post-transition occupancy that j would assume if its proposal were *rejected*). The set of *all* the scenarios constructed in this way represents a "mixed intermediate state": it is *intermediate* because it stays in between the departure and destination state of every cell in the system, and it is *mixed* because it contains information from different scenarios, in each of which every cell assumes its departure state or its arrival state—this will become much clearer when we discuss how the states taking part in different scenarios are combined together to provide a unique value for the acceptance of the transition proposed by every cell.

(*iii*) *Mixing scenarios to get an average acceptance via a local optimization process.* Let us picture the cells as entities that can communicate information. At this stage, i has selected at random d neighboring cells; such d neighboring cells inform i about their transition proposals, so that i can now elaborate the list of possible neighborhood scenarios. However, up to now i knows nothing else; as far as i knows now, all the scenarios around it are equiprobable:

$$p^{(0)}(\boldsymbol{\sigma}_{ik}) = \frac{1}{2^d}, \quad \forall k, \tag{2}$$

where the superscript "(0)" can be conveniently read as "in the first instance." The very same reasoning applies to all the cells in the system.

Let us suppose that in the neighborhood of i the transitions in the kth scenario are accepted, and that the transition proposed by i is also accepted; then the potential involving i in such a case is

$$E_{ik}(n_i + \Delta_i) = -(n_i + \Delta_i)\mu + \varepsilon(n_i + \Delta_i) + \sum_{j=1}^{d} \phi_{X_j}(n_i + \Delta_i, \sigma_{ikj}), \tag{3}$$

where X_j is either neighborhood class A or B, depending on whether the jth neighbor of i shares with i an edge or a corner.

Let us now suppose that the kth scenario is again accepted, but that the transition proposal made by i is rejected; if this is the case, then the potential involving i is

$$E_{ik}(n_i) = -n_i\mu + \varepsilon(n_i) + \sum_{j=1}^{d} \phi_{X_j}(n_i, \sigma_{ikj}).$$

On cell i, the acceptance probability "in the first instance" is

$$\alpha_i^{(0)} = \sum_k p^{(0)}(\boldsymbol{\sigma}_{ik}) A_{ik}(n_i \to n_i + \Delta_i), \tag{4}$$

where $A_{ik}(n_i \to n_i + \Delta_i)$ is the acceptance of transformation $n_i \to n_i + \Delta_i$ on cell i according to the kth scenario. By following a Barker-like approach [43], we can define [let us introduce β as an inverse temperature, $\beta = (k_B T)^{-1}$, where k_B is Boltzmann's constant]

$$A_{ik}(n_i \to n_i + \Delta_i) = \frac{e^{-\beta E_{ik}(n_i + \Delta_i)}}{e^{-\beta E_{ik}(n_i + \Delta_i)} + e^{-\beta E_{ik}(n_i)}}; \tag{5}$$

alternatively, if we follow a Metropolis-Hastings-like approach (MH),

$$A_{ik}(n_i \to n_i + \Delta_i) = \min(1, e^{-\beta[E_{ik}(n_i + \Delta_i) - E_{ik}(n_i)]}). \tag{6}$$

Rejection probability in the first instance is $1 - \alpha_i^{(0)}$. At this stage, unrealistic values like $n_i + \Delta_i = -1$ or $K + 1$ are automatically rejected, since in such cases $E_{ik}(n_i + \Delta_i) = \infty$.

Now cell i knows something more than before: the acceptance of its transition proposal, in the first instance. In particular, in the neighborhood of i we have that every cell j (with $j = 1, \ldots, d$) has its transition proposal accepted with probability $\alpha_j^{(0)}$ or rejected with probability $1 - \alpha_j^{(0)}$. Now, the neighbors of i communicate to i their respective acceptances in the first instance: regarding each and every scenario k, the first tells in the kth scenario, my transition proposal is accepted with probability $\alpha_1^{(0)}$, and negated with probability $1 - \alpha_1^{(0)}$, the second one tells in the kth scenario, my transition proposal is accepted with probability $\alpha_2^{(0)}$, and negated with probability $1 - \alpha_2^{(0)}$, and so on. Therefore, as far as i knows up to now, in its neighborhood each cell j has its respective transition proposal accepted or rejected with probability

$$\gamma_{j,k}^{(1)} = \begin{cases} \alpha_j^{(0)} & \text{(accepted)}, \\ 1 - \alpha_j^{(0)} & \text{(rejected)}, \end{cases} \tag{7}$$

in the first instance. Therefore, as far as i knows now, the kth scenario in its neighborhood is realized with probability

$$p^{(1)}(\boldsymbol{\sigma}_{ik}) = \prod_{j=1}^{d} \gamma_{j,k}^{(1)}. \tag{8}$$

Now, since i sees $p^{(1)}(\boldsymbol{\sigma})$ as the probability that each possible neighborhood scenario $\boldsymbol{\sigma}$ is realized, the acceptance probability for the transformation $n_i \to n_i + \Delta_i$ is, "in the second instance,"

$$\alpha_i^{(1)} = \sum_k p^{(1)}(\boldsymbol{\sigma}_{ik}) A_{ik}(n_i \to n_i + \Delta_i), \tag{9}$$

whereas the rejection probability in the second instance is $1-\alpha_i^{(1)}$. So, this constitutes a first refinement in the determination of the probability that the transition proposed by i will be accepted or not.

Now i knows that every one of the d neighbors it selected has its transition proposal accepted or rejected with probability

$$\gamma_{j,k}^{(2)} = \begin{cases} \alpha_j^{(1)} & \text{(accepted)}, \\ 1-\alpha_j^{(1)} & \text{(rejected)}, \end{cases} \tag{10}$$

in the second instance. Therefore, as far as i knows, the kth neighborhood scenario can happen with probability

$$p^{(2)}(\boldsymbol{\sigma}_{ik}) = \prod_{j=1}^{d} \gamma_{j,k}^{(2)}, \tag{11}$$

and the probability that $n_i \to n_i + \Delta_i$ is accepted is, "in the third instance,"

$$\alpha_i^{(2)} = \sum_k p^{(2)}(\boldsymbol{\sigma}_{ik}) A_{ik}(n_i \to n_i + \Delta_i), \tag{12}$$

whereas the rejection in the third instance is $1-\alpha_i^{(2)}$. We proceed with iterating until the optimization process converges. We indicate as $\alpha_i^{(c)}$ the acceptance probability once the process has converged; it is according to such a probability that we determine whether the transition proposal made by i is accepted or not. At this point, the state of i is updated.

This optimization process, and the subsequent updating of the cells states, proceeds in the very same way simultaneously in all the cells in the system. Once all the states are updated, the time step is completed and the process starts again at (a) with a new time step.

Let us remark that the equation

$$\alpha_i^{(c)} = \sum_k p^{(c)}(\boldsymbol{\sigma}_{ik}) A_{ik}(n_i \to n_i + \Delta_i) \tag{13}$$

can be rewritten as

$$\alpha_i^{(c)} = \langle A_i(n_i \to n_i + \Delta_i) \rangle_I, \tag{14}$$

where I indicates the "mixed intermediate state." In other words, the probability that the transition proposal made by each cell is accepted is the acceptance averaged over all the scenarios that take part in the mixed intermediate state.

Before we proceed to the computational experiment, let us briefly discuss the two crucial features of this algorithm that categorize it as a cellular automaton rule, i.e., *locality* and *synchronicity* (we will not discuss further the conditions of *homogeneity* and *discreteness* because they are satisfied by construction, since the automaton space is a lattice of cells, which is discrete, and the cell states as we defined them are also discrete) [1].

During operation (a) (transition proposals), every cell proposes a trial change of its occupation state; such a proposal is totally independent of the proposals made by the neighbors of that cell; since this is true for *all* the cells in the system, every one of them carries out its own proposal independently (hence, synchronously). During operations $(b)+(c)$ (construction of mixed intermediate states and local optimizations), every cell constructs its own set of neighborhood scenarios, on the basis of which it calculates an average acceptance for the trial occupancy change it proposed (for itself) during operation (a); again, none of these operations depends on what happens in the rest of the system—therefore, operations $(b)+(c)$ are to be carried out independently (hence, synchronously) on each cell.

In light of these observations, the sampling strategy we described in this section is a CA rule because it consists of two *local* operations, each of which is applied to every cell *independently* of all the other cells in the system—and when it goes together with locality, independence implies *synchronicity*, since local, independent operations can be carried out *synchronously*.

IV. COMPUTATIONAL EXPERIMENT

In this section, we report the results of simulations carried out on a lattice as described in Sec. II. CA results are compared with results of standard MC simulations performed with the Metropolis-Hastings technique. The energy parameters [see Eq. (1)] were set in such a way as to get nontrivial occupancy distributions. To this aim, we introduced the following "Lennard-Jones-like" model of interactions:

$$f_{\xi,\sigma,a,\widetilde{x},\pi_1,\pi_2}(x) = \xi\left[\left(\frac{\sigma}{a(\widetilde{x}-x)}\right)^{\pi_1} - \left(\frac{\sigma}{a(\widetilde{x}-x)}\right)^{\pi_2} - \left(\frac{\sigma}{a\widetilde{x}}\right)^{\pi_1} + \left(\frac{\sigma}{a\widetilde{x}}\right)^{\pi_2}\right]. \tag{15}$$

For self-interactions, the function $\varepsilon(n)$ was defined as

$$\varepsilon(n) = \begin{cases} f_{\xi,\sigma,a,\widetilde{x},\pi_1,\pi_2}(n) & \text{if } 0 \leqslant n \leqslant K, \\ \infty & \text{otherwise}, \end{cases}$$

with $K=15$, $\xi = 10$ kJ/mol, $\sigma = 1$, $a = 0.08$, $\widetilde{x} = 20$, $\pi_1 = 12$, and $\pi_2 = 6$. For pair interactions, functions $\phi_A(n,m)$ and $\phi_B(n,m)$ (one for each neighborhood class) were set as

$$\phi_A(n,m) = \begin{cases} f_{\xi,\sigma,a,\widetilde{x},\pi_1,\pi_2}(n+m) & 0 \leqslant n,m \leqslant K, \\ \infty & \text{otherwise} \end{cases}$$

with $K=15$, $\xi = 40$ kJ/mol, $\sigma = 1$, $a = 0.08$, $\widetilde{x} = 40$, $\pi_1 = 12$, and $\pi_2 = 6$ for class A, and

$$\phi_B(n,m) = \begin{cases} f_{\xi,\sigma,a,\widetilde{x},\pi_1,\pi_2}(n+m), & 0 \leqslant n,m \leqslant K, \\ \infty & \text{otherwise}, \end{cases}$$

with $K=15$, $\xi = 30$ kJ/mol, $\sigma = 1$, $a = 0.08$, $\widetilde{x} = 40$, $\pi_1 = 12$, and $\pi_2 = 6$ for class B. Temperature was set to the indicative value of $T = 300$ K.

The system was made of a square lattice of 64 cells, and simulated for 41 values of chemical potential, equally spaced in the interval between -3 and 3 kJ/mol, both in grand-canonical MC (GCMC) simulations and in CA simulations. For CA simulations, both Barker-acceptance and MH-acceptance variants were explored. To carry out comparisons also in terms of efficiency in the decay of cell occupancy fluctuations, GCMC simulations were carried out according to the following procedure: for each sweep, all the cells were picked in a random sequence; each cell, e.g., cell i, was given the chance to propose a trial transition, $\Delta_i = +1$ or -1, with uniform probability; the trial potential was then

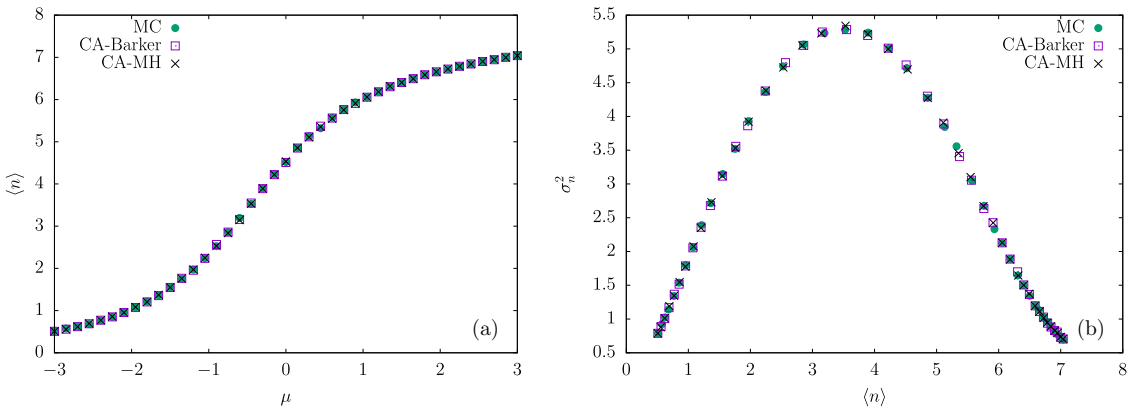

FIG. 1. Adsorption isotherm (a) and variance vs the loading (b). Chemical potential units are kJ/mol.

calculated,

$$E_i(n_i + \Delta_i) = -(n_i + \Delta_i)\mu + \varepsilon(n_i + \Delta_i) + \sum_{j=1}^{\nu} \phi_{X_j}(n_i + \Delta_i, n_j), \tag{16}$$

and compared with the potential on cell i right before the trial transition,

$$E_i(n_i) = -n_i\mu + \varepsilon(n_i) + \sum_{j=1}^{\nu} \phi_{X_j}(n_i, n_j),$$

through evaluation of the potential difference $\Delta E_i = E_i(n_i + \Delta_i) - E_{ik}(n_i)$; the proposed transition was accepted with probability (MH approach) $\alpha_i = \min[1, \exp(-\beta \Delta E_i)]$, or rejected with probability $1 - \alpha_i$.

For each variant of the CA model, we also investigated all the possible values of d, i.e., the number of randomly picked neighbors that at each time step take part in the neighborhood scenario of each cell; the results we obtained were the same. For each chemical potential value, every simulation was performed over 10^5 postequilibration steps. We considered the optimization procedure [described in paragraph *(c)* in Sec. III] converged once the variation in the acceptance probability was less than the threshold 10^{-6}; in each simulation, we observed that the optimization procedure always required a number of iterations between 3 and 5.

In Fig. 1(a), we show the adsorption isotherms, i.e., the stationary average cell occupancy (also called the *coverage* or the *loading*) as a function of the chemical potential. The agreement between CA and MC simulations is nearly perfect. Small discrepancies become more visible in the plot of occupancy variance, Fig. 1(b)—fluctuations are not reproduced with the same accuracy as the loading, but the agreement is quantitative anyway. In particular, a small discrepancy is noticed between the two CA variants, meaning that the two

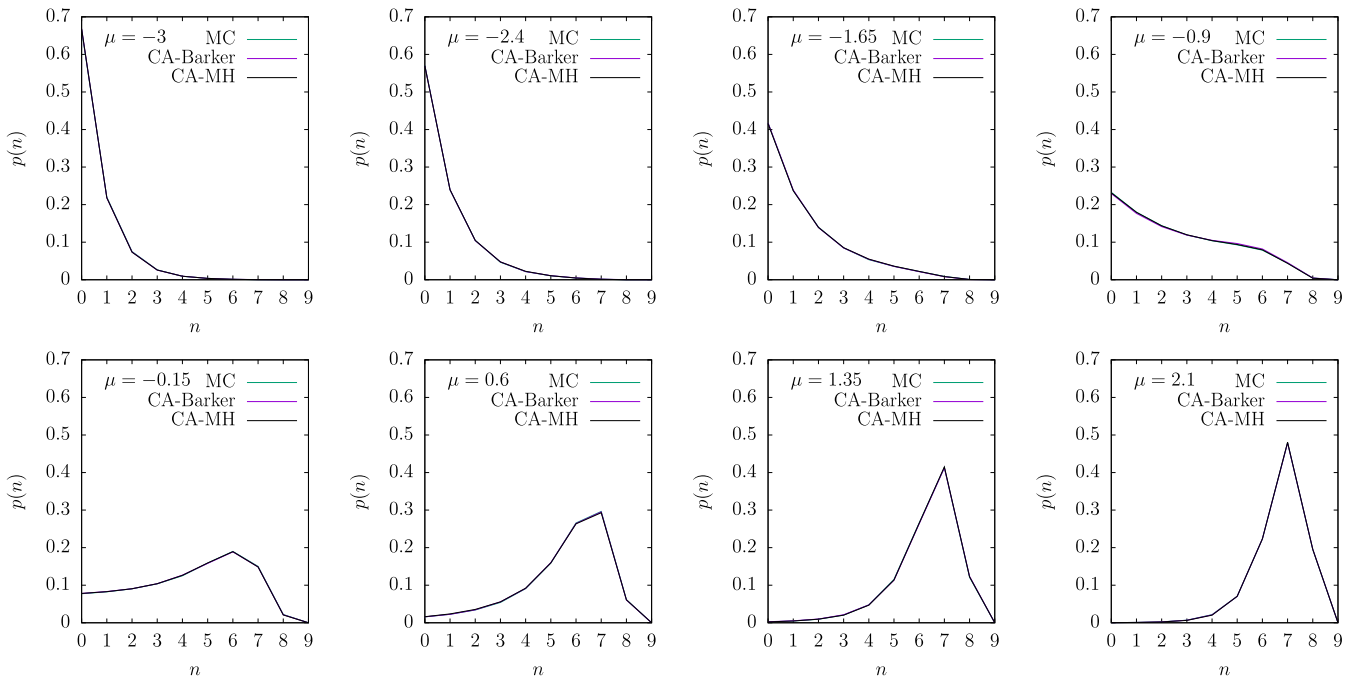

FIG. 2. Self-occupancy distributions. Chemical potential units are kJ/mol.

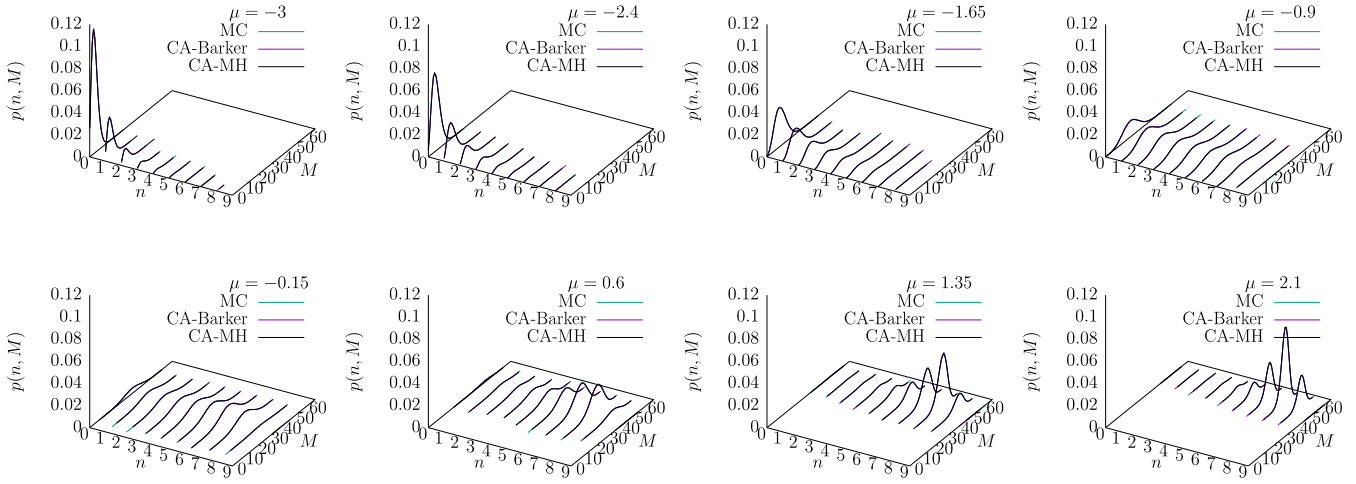

FIG. 3. Joint self-neighborhood distributions. Chemical potential units are kJ/mol.

approaches (Barker acceptance and MH acceptance) converge towards slightly different stationary states.

However, both methods are in very good agreement with MC results. This is confirmed by the perfect overlapping between the cell occupancy distribution plots shown in Figs. 2 and 3. In Fig. 2 we report the stationary probability, $p(n)$, that a cell has occupancy n, at eight selected values of chemical potential. In Fig. 3 we report the joint probability, $p(n, M)$, that a cell has occupancy n and that, at the same time, the sum of neighboring occupancies is M—the remarkable overlapping shows that local distributions and local correlations are respected.

To get an idea of how efficient this model is in leading cell occupancies towards stationarity, we investigated the autocorrelation function of cell occupancy fluctuations,

$$\Phi(t) = \frac{\langle \delta n(t) \delta n(0) \rangle}{\langle \delta n(0)^2 \rangle}, \tag{17}$$

where t is a fictitious time (it is really the number of steps), and $\delta n(t) = n(t) - \langle n \rangle$. In Fig. 4 we show the obtained decays at chemical potential $\mu = -0.15$ kJ/mol for MC and for the two CA variants. As expected, the automaton in "Barker mode" retains memory of the previous state for a longer time; this is due to the mathematical formulation of acceptance [see Eq. (5)], less efficient than MH [Eq. (6)]. In MH mode, the automaton relaxes in the same way as in Metropolis-Hastings MC—Metropolis-Hastings, in turn, is the most efficient MC sampling technique [44], Another interesting feature we can notice from Fig. 4 is that, contrary to our expectations, the model is relatively insensitive to the number of neighbors considered during the creation of neighborhood scenarios. This is somewhat surprising, since we thought that, despite being more computationally expensive, a larger number of contributions in the mixed intermediate states could lead to a better approximation of the reference model, and to a faster relaxation of cell fluctuations. Instead, this behavior leads us to assume that the key trick in our CA formulation is the very fact that an intermediate state is used.

Our CA lacks detailed balance globally (even if it satisfies detailed balance *locally*, as we will show in the next section). This leads us to ask ourselves with which degree of accuracy collective properties are reproduced. To answer this question, we calculated the average energy of adsorption by means of

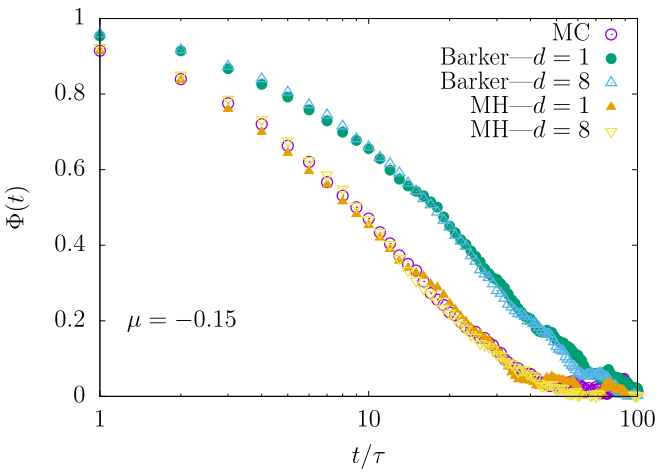

FIG. 4. Decay of fluctuations in the cell occupancy [see Eq. (17)]. Chemical potential units are kJ/mol.

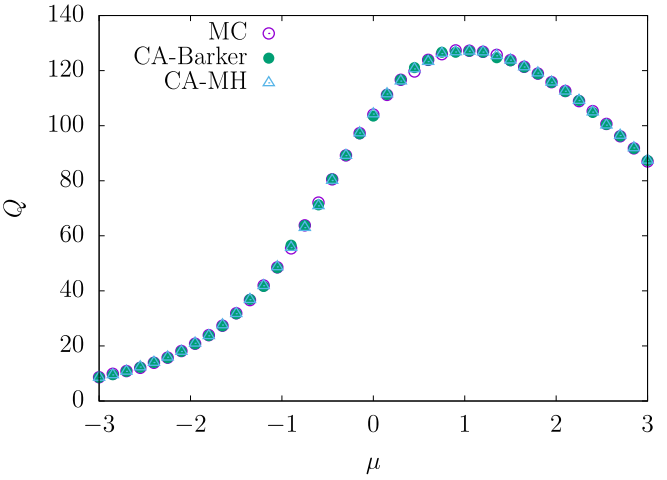

FIG. 5. Average energy of adsorption. Units are kJ/mol.

TABLE I. Forward and backward probability fluxes between occupancies n and n', and their ratios, both in the Barker-like and in the MH-like approach. With this table we want to show that, for both approaches, the ratio between forward and backward probability fluxes is *exactly* unity—we can safely say "exactly" because all the quantities here were calculated in `real(kind=16)` precision from the Chapman-Kolmogorov equation. This allowed us to represent numbers with that many significant digits—we realize that, at first glance, such a representation might seem redundant; however, it is absolutely necessary in this case, because violations of detailed balance ultimately manifest themselves under the form of nonunity ratios (sometimes quasiunity, but definitely nonunity), and the deviations from exact unity can, in many cases, be very subtle (like, e.g., 1.0000014223 rather than 1.0000000000), and they could go undetected if we represented ratios with a smaller number of digits.

		$\mu = -6$ kJ/mol					
		Barker			MH		
n	n'	$p(n, n')$	$p(n', n)$	ratio	$p(n, n')$	$p(n', n)$	ratio
0	0	0.6236587350	0.6236587350	1.0000000000	0.6038370109	0.6038370109	1.0000000000
0	1	0.0737603055	0.0737603055	1.0000000000	0.0935563839	0.0935563839	1.0000000000
1	0	0.0737603055	0.0737603055	1.0000000000	0.0935563839	0.0935563839	1.0000000000
1	1	0.0873897924	0.0873897924	1.0000000000	0.0576092701	0.0576092701	1.0000000000
1	2	0.0259631981	0.0259631981	1.0000000000	0.0359471138	0.0359471138	1.0000000000
2	1	0.0259631981	0.0259631981	1.0000000000	0.0359471138	0.0359471138	1.0000000000
2	2	0.0323608129	0.0323608129	1.0000000000	0.0141473090	0.0141473090	1.0000000000
2	3	0.0135624133	0.0135624133	1.0000000000	0.0217998049	0.0217998049	1.0000000000
3	2	0.0135624133	0.0135624133	1.0000000000	0.0217998049	0.0217998049	1.0000000000
3	3	0.0300188259	0.0300188259	1.0000000000	0.0217998049	0.0217998049	1.0000000000
		$\mu = -3$ kJ/mol					
		Barker			MH		
n	n'	$p(n, n')$	$p(n', n)$	ratio	$p(n, n')$	$p(n', n)$	ratio
0	0	0.1210029987	0.1210029987	1.0000000000	0.0838064898	0.0838064898	1.0000000000
0	1	0.0390626418	0.0390626418	1.0000000000	0.0763155876	0.0763155876	1.0000000000
1	0	0.0390626418	0.0390626418	1.0000000000	0.0763155876	0.0763155876	1.0000000000
1	1	0.0692631041	0.0692631041	1.0000000000	0.0000593667	0.0000593667	1.0000000000
1	2	0.0443724926	0.0443724926	1.0000000000	0.0763749543	0.0763749543	1.0000000000
2	1	0.0443724926	0.0443724926	1.0000000000	0.0763749543	0.0763749543	1.0000000000
2	2	0.0944544704	0.0944544704	1.0000000000	0.0296752077	0.0296752077	1.0000000000
2	3	0.0732814472	0.0732814472	1.0000000000	0.1060501620	0.1060501620	1.0000000000
3	2	0.0732814472	0.0732814472	1.0000000000	0.1060501620	0.1060501620	1.0000000000
3	3	0.4018462635	0.4018462635	1.0000000000	0.3689775280	0.3689775280	1.0000000000

statistical mechanics from the covariance between the total number of molecules and the total energy, divided by the variance in the total number of molecules:

$$Q = \frac{\langle EN\rangle - \langle E\rangle\langle N\rangle}{\langle N^2\rangle - \langle N\rangle^2}. \tag{18}$$

However, the exact expression for the energy of the automaton is unknown; this is because we could not express the CA stationary distribution in a closed form, and therefore we have no access to the relative pseudo-Hamiltonian. Therefore we used, as an approximate measure for the total energy, the total interaction energy of the reference system, i.e., $E = \Omega_{\text{tot}} + \mu N$, with Ω_{tot} given by Eq. (1). As we can see from Fig. 5, also in this case the agreement is quantitative, meaning that, despite the lack of detailed balance, also the collective properties can be calculated and provide results in very good agreement with the grand-canonical ensemble.

V. LOCAL BALANCE

As we already mentioned, our CA does not satisfy detailed balance globally. Nevertheless, what we found in all our numerical simulations is that a *local detailed balance* is satisfied—by "local" we mean cellwise: if we consider the joint probability $p(n, n')$ of a cell to have occupancy n and, in the next step, to have occupancy n', it happens that

$$\frac{p(n, n')}{p(n', n)} = 1, \tag{19}$$

with a deviation from unity that decreases as the number of steps increases. Besides such evidence, which comes from numerical simulations, we implemented the exact computation of the CA transition matrix for a one-dimensional system made up of four cells with periodic boundary conditions for different sets of energy parameters, and we used the Chapman-Kolmogorov equation to get the stationary distributions.

In Table I we report the results about forward and backward fluxes, calculated exactly, for every pair of occupancies in a

one-dimensional system parametrized as follows: with regard to self-interactions,

$$\varepsilon(n) = \begin{cases} f_{\xi,\sigma,a,\widetilde{x},\pi_1,\pi_2}(n) & \text{if } 0 \leqslant n \leqslant K, \\ \infty & \text{otherwise,} \end{cases}$$

with $K = 3$, $\xi = 120$ kJ/mol, $\sigma = 1$, $a = 0.08$, $\widetilde{x} = 20$, $\pi_1 = 12$, $\pi_2 = 6$, whereas with regard to pair-interactions (in a one-dimensional system we have only one neighborhood class),

$$\phi(n, m) = \begin{cases} f_{\xi,\sigma,a,\widetilde{x},\pi_1,\pi_2}(n+m), & 0 \leqslant n, m \leqslant K. \\ \infty, & \text{otherwise,} \end{cases}$$

with $K = 3$, $\xi = 1500$ kJ/mol, $\sigma = 1$, $a = 0.08$, $\widetilde{x} = 40$, $\pi_1 = 12$, and $\pi_2 = 6$. Also in this case, the temperature was set to the indicative value of $T = 300$ K. From transition matrices we verified that, despite the lack of global detailed balance, Eq. (19) (i.e., local detailed balance) is always verified *exactly*. This can be seen very clearly in columns five and eight of Table I, where we report the ratio between forward and backward occupancy transition probabilities calculated *exactly* from the Chapman-Kolmogorov equation, respectively, for the Barker approach, and for the Metropolis-Hastings approach.

We already noticed in Sec. IV that the CA simulation outcomes differ slightly depending on whether a Barker-like or a MH-like acceptance approach is used. In Table II we report a comparison between the distribution calculated exactly for the one-dimensional system according to both approaches; results confirm that it is actually true that the two methods provide slightly different results.

VI. DISCUSSION

As we already mentioned, we could not obtain a closed form for the stationary distribution of occupancies produced by the algorithm. Nevertheless, here we would like to discuss the CA evolution rule, especially with regard to the use of mixed intermediate states and their role in the local balance.

In a previous attempt to formulate the CA model, we did not make use of any intermediate state: acceptance was computed on the basis of all possible neighborhood scenarios irrespective of the transition proposal made by each cell: in other words, acceptance was averaged over all the possible neighborhood occupancies that could happen after an occupancy change -1, 0, and $+1$; the resulting model did not satisfy detailed balance either globally or locally.

In another attempt, while we introduced the mixed intermediate state, the scenario probabilities in the first instance, Eq. (2), were not computed at all; the evolution rule skipped it and prescribed directly the calculation of acceptance in the first instance, Eq. (4), which was not computed by averaging over the possible neighborhood scenarios, but rather on the basis of the occupancies in the neighboring cells at the beginning of the time step. Also in this case the resulting model did not satisfy detailed balance in any form, since the neighborhood scenarios were associated with probabilities that differ depending on whether we accessed the intermediate state from the departure or the arrival configuration. Therefore, it is reasonable to assume that local detailed balance is due to (i) the use of a mixed intermediate state for each cell, (ii) the fact that such an intermediate state can be reached with

TABLE II. Occupancy distributions for the one-dimensional system (numerically) solved exactly. As in Table I, here we make use of a number of significant digits that, at first glance, might appear redundant. However, our scope with this table is to show that, although the rule satisfies local detailed balance as shown in Table I, the stationary properties show a mild dependence on the particular form we chose for the acceptance (in this paper, Barker-like or Metropolis-Hastings-like); such dependence might go unnoticed if we represented average occupancies and probability distributions with a smaller number of digits.

	$\mu = -6$ kJ/mol	
	Barker $\langle n \rangle = 0.461630$	MH $\langle n \rangle = 0.461700$
n	$p(n)$	$p(n)$
0	0.697419	0.697393
1	0.187113	0.187113
2	0.071886	0.071894
3	0.043581	0.043600
	$\mu = -4.8$ kJ/mol	
	Barker $\langle n \rangle = 0.926805$	MH $\langle n \rangle = 0.926961$
n	$p(n)$	$p(n)$
0	0.497526	0.497474
1	0.220174	0.220160
2	0.140269	0.140295
3	0.142031	0.142070
	$\mu = -3.8$ kJ/mol	
	Barker $\langle n \rangle = 1.518773$	MH $\langle n \rangle = 1.518735$
n	$p(n)$	$p(n)$
0	0.295047	0.295055
1	0.199915	0.199917
2	0.196258	0.196267
3	0.308780	0.308761
	$\mu = -3$ kJ/mol	
	Barker $\langle n \rangle = 2.002298$	MH $\langle n \rangle = 2.002034$
n	$p(n)$	$p(n)$
0	0.160066	0.160122
1	0.152698	0.152750
2	0.212108	0.212100
3	0.475128	0.475028
	$\mu = -2$ kJ/mol	
	Barker $\langle n \rangle = 2.445069$	MH $\langle n \rangle = 2.444913$
n	$p(n)$	$p(n)$
0	0.061628	0.061661
1	0.089651	0.089675
2	0.190744	0.190753
3	0.657977	0.657911

TABLE II. (*Continued.*)

	$\mu = 1$ kJ/mol	
	Barker $\langle n \rangle = 2.895964$	MH $\langle n \rangle = 2.895962$
n	$p(n)$	$p(n)$
0	0.002120	0.002120
1	0.010516	0.010516
2	0.076643	0.076644
3	0.910721	0.910719

the same probability both from the departure and the arrival configuration, and (iii) the probability of each neighborhood scenario being the same regardless of the fact that we entered the mixed intermediate state from the departure or from the arrival configuration.

To clarify what we mean when we talk about "accessing the mixed intermediate state with the same probability," let us examine the path that the system has to walk in order to get back from the configuration it just reached to the previous one. We want each cell to have the chance to return back to its previous occupancy by passing through the same mixed intermediate state it just visited. In other words, we are considering the system right after the transformation $A \to I \to B$, and we want it to get back to A through $B \to I \to A$. The cells that transformed from A to B while having their transition proposal accepted, i.e., $\Delta_i = +1$ ($\Delta_i = -1$), need to select the opposite transition, i.e., $\Delta_i = -1$ ($\Delta_i = +1$) in order to access the same intermediate state as before; the ones that had their transition proposal rejected need instead to select the same transition. Now, since $q^{(+)} = q^{(-)}$, the probability of $B \to I$ is the same as the probability of $A \to I$. Once they reached the same mixed intermediate state as before, since the optimization procedure starts from the same conditions [Eq. (2)] and is carried out over the same scenarios, also the probability distributions $p^{(0)}(\boldsymbol{\sigma}_{ik})$, $p^{(1)}(\boldsymbol{\sigma}_{ik})$, $\ldots$, $p^{(c)}(\boldsymbol{\sigma}_{ik})$ are the same as those we encountered along the path $A \to I \to B$.

While the use of mixed intermediate states is very likely to be the only reason why local detailed balance is obeyed, the role played by the optimization procedure instead is merely that of improving the agreement between the CA distribution and their MC counterparts. A crucial role is then played by the way we define acceptances; we showed that both the Barker-like and MH-like approaches effectively lead the system towards stationary distributions in very good agreement with the reference MC model, the only difference between these two approaches being that the MH version of the CA allows for a faster equilibration, similar to what happens in asynchronous MC methods.

VII. CONCLUSIONS

We constructed a cellular automaton that satisfies local detailed balance and provides stationary cell occupancy distributions in very good agreement with their Monte Carlo counterparts. A key role is played by the use of "mixed intermediate states," i.e., intermediate situations where the acceptance of trial moves is determined on the basis of a number of possible outcoming states in the neighborhood of each cell. This approach can successfully be used in occupancy-based models, and its main advantage is the fact that the resulting automaton is fully synchronous, thus constituting a parallelizable alternative to sequential MC. The key role played by the mixed intermediate state needs further investigation, in particular in the generalization of this approach to particle-based lattice-gas simulations. We believe that the synchronous sampling strategy we developed here contributes to taking a stone off the wall that separates us from knowing more about the coexistence between full synchronicity, nontrivial interactions, and detailed balance, and it could be taken as the starting point of a line of research centered around probabilistic cellular automata and their role in the modeling of systems *at thermodynamic equilibrium*.

ACKNOWLEDGMENTS

F.G.P. is thankful to the Regione Autonoma della Sardegna for the Contract "Ricercatore a Tempo Determinato," financed through the resources of POR—FSE 2014-2020—Asse Prioritario 3 "Istruzione e Formazione"—Obiettivo tematico: 10, Priorità di investimento: 10ii, Obiettivo specifico: 10,5, Azione dell'Accordo di Paternariato 10.5.12—C.U.P. J86C18000270002.

[1] B. Chopard and M. Droz, *Cellular Automata Modeling of Physical Systems*, 1st ed. (Cambridge University Press, Cambridge, England, 1998).

[2] S. Wolfram, *A New Kind of Science* (Wolfram Media, 2002).

[3] J. P. Boon, D. Dab, R. Kapral, and A. T. Lawniczak, Lattice gas automata for reactive systems, Phys. Rep. **273**, 55 (1996).

[4] N. Israeli and N. Goldenfeld, Coarse-graining of cellular automata, emergence, and the predictability of complex systems, Phys. Rev. E **73**, 026203 (2006).

[5] T. Toffoli and N. Margolus, *Cellular Automata Machines: A New Environment for Modeling*, 1st ed. (MIT Press, Cambridge, MA, 1997).

[6] P. J. Hoogerbrugge and J. M. V. A. Koelman, Simulating microscopic hydrodynamic phenomena with dissipative particle dynamics, Europhys. Lett. **19**, 155 (1992).

[7] J. M. V. A. Koelman and P. J. Hoogerbrugge, Dynamic simulations of hard-sphere suspensions under steady shear, Europhys. Lett. **21**, 363 (1993).

[8] P. Español and P. Warren, Statistical mechanics of dissipative particle dynamics, Europhys. Lett. **30**, 191 (1995).

[9] D. Wolf-Gladrow, *Lattice-Gas Cellular Automata and Lattice Boltzmann Models* (Springer-Verlag, Berlin, 2000).

[10] S. Succi, *The Lattice Boltzmann Equation for Fluid Dynamics and Beyond* (Oxford University Press, Oxford, England, 2001).

[11] W. A. Little, The existence of persistent states in the brain, Math. Biosci. **19**, 101 (1974).

[12] P. Peretto, Collective properties of neural networks: A statistical physics approach, Biol. Cybern. **50**, 51 (1984).

[13] S. Goldstein, R. Kuik, J. L. Lebowitz, and C. Maes, From PCA's to equilibrium systems and back, Commun. Math. Phys. **125**, 71 (1989).
[14] H. Föllmer and U. Horst, Convergence of locally and globally interacting Markov chains, Stoch. Proc. Appl. **96**, 99 (2001).
[15] F. G. Pazzona, P. Demontis, and G. B. Suffritti, Conciliating synchronicity with spatial discretization, exclusion, interactions, and detailed balance, Phys. Rev. E **88**, 062114 (2013).
[16] B. Chopard, L. Frachebourg, and M. Droz, Multiparticle lattice gas automata for reaction-diffusion systems, Int. J. Mod. Phys. C **05**, 47 (1994).
[17] A. Masselot and B. Chopard, A multiparticle lattice-gas model for hydrodynamics, Int. J. Mod. Phys. C **09**, 1221 (1998).
[18] J. Güémez, S. Velasco, and A. Calvo Hernández, Probability distribution for a lattice gas model: I. General study, Physica A **152**, 226 (1988).
[19] J. Güémez, S. Velasco, and A. Calvo Hernández, Probability distribution for a lattice gas model: II. Thermodynamic limit, Physica A **152**, 243 (1988).
[20] T. T. P. Cheung, Probability distribution in the cell theory of an interacting lattice gas: Application to ^{129}Xe NMR of xenon in zeolites, J. Phys. Chem. **97**, 8993 (1993).
[21] S. Ma, Renormalization group by Monte Carlo methods, Phys. Rev. Lett. **37**, 461 (1976).
[22] M. Katsoulakis and D. G. Vlachos, Mathematical strategies for the coarse-graining of microscopic models, in *Handbook of Materials Modeling*, edited by S. Yip (Springer, Dordrecht, 2005), pp. 1477–1490.
[23] M. Katsoulakis, A. J. Majda, and D. G. Vlachos, Coarse-grained stochastic processes for microscopic lattice systems, Proc. Natl. Acad. Sci. (USA) **100**, 782 (2003).
[24] A. Chatterjee, D. G. Vlachos, and M. Katsoulakis, Spatially adaptive lattice coarse-grained Monte Carlo simulations for diffusion of interacting molecules, J. Chem. Phys. **121**, 11420 (2004).
[25] J. Dai, W. D. Seider, and T. Sinno, Coarse-grained lattice kinetic Monte Carlo simulation of systems of strongly interacting particles, J. Chem. Phys. **128**, 194705 (2008).
[26] X. Liu, W. D. Seider, and T. Sinno, Coarse-grained lattice Monte Carlo simulations with continuous interaction potentials, Phys. Rev. E **86**, 026708 (2012).
[27] M. Katsoulakis and P. Plecháč, Coarse-graining schemes for stochastic lattice systems with short and long-range interactions, Math. Comp. **83**, 1757 (2014).
[28] J. J. de la Torre and P. Español, Coarse-graining Brownian motion: From particles to a discrete diffusion equation, J. Chem. Phys. **135**, 114103 (2011).
[29] C. Tunca and D. Ford, A transition-state theory approach to adsorbate dynamics at arbitrary loadings, J. Chem. Phys. **111**, 2751 (1999).
[30] C. Tunca and D. Ford, Modeling cage-to-cage dynamics of adsorbates at arbitrary loadings with dynamically corrected transition-state theory, J. Phys. Chem. B **106**, 10982 (2002).
[31] C. Tunca and D. Ford, A hierarchical approach to the molecular modeling of diffusion and adsorption at nonzero loading in microporous materials, Chem. Eng. Sci. **58**, 3373 (2003).
[32] C. Tunca and D. Ford, Coarse-grained nonequilibrium approach to the molecular modeling of permeation through microporous membranes, J. Chem. Phys. **120**, 10763 (2004).
[33] F. G. Pazzona, P. Demontis, and G. B. Suffritti, Synchronous equilibrium model for the diffusion of mutually exclusive particles in a heterogeneous lattice of adsorption site, Phys. Rev. E **87**, 063306 (2013).
[34] F. G. Pazzona, G. Pireddu, A. Gabrieli, A. M. Pintus, P. Demontis, and G. B. Suffritti, Local free energies for the coarse-graining of adsorption phenomena: The interacting pair approximation, J. Chem. Phys. **148**, 194108 (2018).
[35] G. Pireddu, F. G. Pazzona, A. M. Pintus, A. Gabrieli, and P. Demontis, Spatial coarse-graining of methane adsorption in graphene materials, J. Phys. Chem. C **123**, 18355 (2019).
[36] G. Pireddu, F. G. Pazzona, P. Demontis, and M. A. Załuska-Kotur, Scaling-up simulations of diffusion in microporous materials, J. Chem. Theor. Comput. **15**, 6931 (2019).
[37] E. Alerstam, T. Svensson, and S. Andersson-Engels, Parallel computing with graphics processing units for high-speed Monte Carlo simulation of photon migration, J. Biomed. Opt. **13**, 060504 (2008).
[38] J. C. Phillips *et al.*, Scalable molecular dynamics on CPU and GPU architectures with NAMD, J. Chem. Phys. **153**, 044130 (2020).
[39] M. Weigel, Monte Carlo methods for massively parallel computers, in *Order, Disorder and Criticality*, edited by Y. Holovatch (World Scientific, Singapore, 2018), Vol. 5, pp. 271–340.
[40] R. H. Swendsen and J.-S. Wang, Nonuniversal Critical Dynamics in Monte Carlo Simulations, Phys. Rev. Lett. **58**, 86 (1987).
[41] W. G. Kranendonk and D. Frenkel, Simulation of the adhesive-hard-sphere model, Mol. Phys. **64**, 403 (1988).
[42] F. G. Pazzona, P. Demontis, and G. B. Suffritti, Improving the acceptance in Monte Carlo simulations: Sampling through intermediate states, J. Comput. Phys. **295**, 556 (2015).
[43] A. A. Barker, Monte Carlo calculations of the radial distribution functions for a proton-electron plasma, Aust. J. Phys. **18**, 119 (1965).
[44] P. H. Peksun, Optimum Monte-Carlo sampling using Markov chains, Biometrika **60**, 607 (1973).